can get an exact expression, instead of an upper limit for the effect of one intermediate photon by refining the above arguments in an obvious way. The result is then the analogue of Bhabha-Heitler's Eq. (23) for $n=1$, but it involves multiple integrals which cannot be evaluated easily and it is probably not worth writing down, since the effect it describes is so small.

The author would like to thank the U. S. Atomic Energy Commission for a fellowship during the tenure of which this work was done.

PHYSICAL REVIEW VOLUME 77, NUMBER 1 JANUARY 1, 1950

Dimensional Effects Resulting from a High Dielectric Constant Found in a Ferromagnetic Ferrite

FRANK G. BROCKMAN, P. H. DOWLING, AND WALTER G. STENECK
Philips Laboratories, Inc., Irvington-on-Hudson, New York

(Received September 6, 1949)

A variety of a ferromagnetic ferrite is shown to have dielectric properties corresponding to a dielectric constant of the order of 10^5. Coupled with a magnetic permeability of about 10^3, this leads to dimensional resonance effects such that the apparent permeability of a core whose section is 2.5×1.25 cm reduces to very low values in the region of 2 megacycles. An apparent anomaly exists in the dielectric behavior in the vicinity of the magnetic Curie point. A general theory of dimensional effects encountered in measuring magnetic and dielectric constants is developed. This theory is based on the geometry of the infinite slab. When the theory is applied to the ferrite under study, a residual variation of the permeability with frequency remains, which may be explained by magnetic resonance. The theory accounts adequately for the dielectric effects at the Curie point.

I. INTRODUCTION

IN the last few years there was developed in the Philips Laboratories, in Eindhoven, Holland, a series of non-metallic ferromagnetic materials by Snoek, Verwey and their coworkers.[1] Being non-metallic these materials have low electrical conductivity and therefore low eddy current losses when used in an alternating magnetic field. Because of this development, Philips Laboratories, Irvington, New York, were consulted regarding the use of one of these materials in the construction of a special massive ferromagnetic core for use in the lower megacycle region. The chief requirements made of the core material were as high permeability as possible (preferably not less than 1000) together with low losses (hysteresis and residual losses as well as eddy current loss) at frequencies up to 5 megacycles per second. Aside from the problem of the choice of the material based on the magnetic properties, there also existed the purely mechanical problem of the construction of such a core, which would weigh about $\frac{1}{2}$ ton.

One of the commercial varieties of the non-metallic magnetic materials mentioned above is a manganese-zinc ferrite, marketed under the trade mark Ferroxcube III. Consideration of the nominal properties of this material (Table I) indicated that it would probably be acceptable for this application.

Since these materials are not ductile and cannot be cast, it was decided that the large core could be assembled of brick-shaped pieces which would be accurately dimensioned and squared. This latter requirement was imposed to reduce the effects of air gaps in the structure to a minimum.

For preliminary studies a smaller test core was constructed. The sizes chosen for the brick-shaped pieces were $5\times2.5\times1.25$ cm and $10\times2.5\times1.25$ cm. In the core structure these sizes present a minimum dimension, in a direction perpendicular to the magnetic flux, of 1.25 cm. On the basis of the resistivity of the material (Table I) and this dimension, it was estimated that eddy-current losses would not be excessive.

However, when the initial permeability of the bricks was investigated as a function of frequency it was found to decrease rapidly to a very low value at about 2 mc. Because this frequency was considerably lower than had been expected from previous experience, an investigation of the effect was made. This investigation led first to the prediction that the material must possess a dielectric behavior corresponding to an unexpectedly large dielectric constant of the order of 5×10^4 and then to the experimental verification of this fact.

TABLE I. Nominal characteristics of Ferroxcube III.

Initial permeability, μ_0	1000 to 1500
Loss factor, $\tan\delta/\mu_0$, 60 kc	0.1×10^{-4}
Hysteresis resistance coefficient,* 2 kc	1 to 4×10^{-6}
Resistivity	100 ohm cm

* Victor E. Legg, Bell Sys. Tech. J. **15**, 39 (1936).

[1] (a) J. L. Snoek, *New Developments in Ferromagnetic Materials* (Elsevier Publishing Co., New York, 1947). (b) J. L. Snoek, Philips Tech. Rev. **8**, 353 (1946). (c) E. J. W. Verwey, Philips Tech. Rev. **9**, 46 (1947). (d) Verwey, Haayman, and Heilman, Philips Tech. Rev. **9**, 185 (1947). (e) E. J. W. Verwey and E. L. Heilman, J. Chem. Phys. **15**, 174 (1947). (f) Verwey, Haayman, and Romeyn, Philips Tech. Rev. **15**, 181 (1947).

With a permeability of 10^3 and a dielectric constant of 5×10^4, the wave-length of an electromagnetic wave in a core of Ferroxcube III is about 2 cm at 2 megacycles. Dimensional resonance effects may thus be expected at this frequency in a core about 1 cm thick. Furthermore, as the core thickness is decreased, such resonance effects will be pushed to higher frequencies as confirmed by experiment. When dimensional resonance occurs, the real component of the flux decreases to low values or, if the losses be low enough, may pass through zero to negative values. A corresponding variation will be produced in the apparent or effective permeability, thus accounting for the low apparent permeability we found at 2 mc in the bricks of Ferroxcube III.

The origin of the dielectric behavior of Ferroxcube III is not entirely clear. Polder,[2] of the Philips Laboratory, Eindhoven, has advanced an explanation based on a fine-grained texture of this material giving rise to a distribution of barrier layers, and von Hippel has informally suggested a somewhat similar explanation. For large scale measurements such a material will behave as though it had a high dielectric constant, even though it nowhere possesses a significantly large inherent dielectric constant.

When calculations are made according to our theory for the removal of dimensional effects, a considerable dispersion remains in the magnetic permeability so derived. It is possible to account for this, as Snoek[3] has done, by magnetic resonance. His paper contains a misprint for the value of g, the gyromagnetic ratio. When the correct value of 1.76×10^7 is substituted in his formula, the frequency at which the actual permeability of Ferroxcube III reduces to half value comes out to be 1.26×10^7 c.p.s. Our measurements give about 0.5×10^7 for the half value frequency. Snoek has advanced reasons as to why such a discrepancy might be expected.

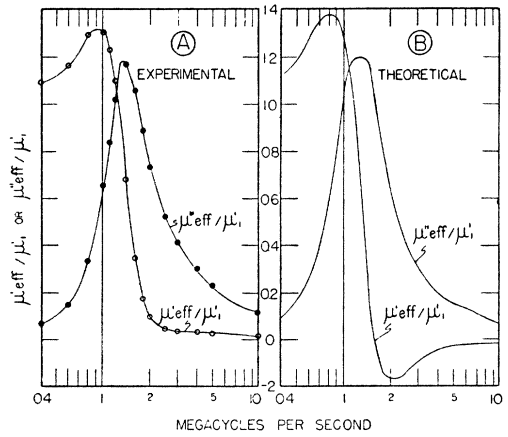

FIG. 1. Core section 2.5×1.25 cm. A. Experimental values of the ratio of the effective permeabilities to the real part of the actual permeability at 1000 c.p.s. B. Theoretical values of the same.

[2] D. Polder, forthcoming publication.
[3] J. L. Snoek, Physica 14, 207 (1948).

II. EXPERIMENTAL

Magnetic Experiments

For the magnetic measurements on the bricks a square core was assembled from two of the 5 cm bricks and two of the 10 cm bricks. The core was thus 10 cm square with a window 5×5 cm. This core was wound with an appropriate number of turns of insulated copper wire and the resulting inductor was measured upon a General Radio Type 916-A Radio Frequency Bridge. The data obtained by these measurements are the equivalent series reactance and resistance between the two terminals of the inductor. This equivalent is the representation usually employed in studies of this kind. The inductance at a low frequency (1000 c.p.s.) was obtained using a General Radio Type 667-A Inductance Bridge. In all cases the current through the measured inductor was kept so small that the measured reactance corresponded to the initial permeability.

At the higher frequencies corrections have been applied for the distributed capacitance. Part of this capacitance, 2.8 mmfd, exists at the Type 916-A bridge terminals and part is due to the winding on the core. This latter value was estimated by preparing a polystyrene duplicate core which was coated, except for a horizontal space to break the eddy current circuit, with a thin layer of Aquadag. A similar winding was applied to this duplicate core and the distributed capacitance evaluated by determining the resonant frequency of this inductor for various values of capacitance using a Boonton Type 160-A Q-meter. By plotting the inverse of the square of the angular resonant frequency against the added capacitance, a straight line relationship is obtained which can be extrapolated to yield a value for the distributed capacitance of the coil.

In Fig. 1A are shown the data on the brick core, plotted as the ratio of the effective permeabilities to the real part of the actual permeability at 1000 c.p.s., i.e., μ_{eff}'/μ_1' and $\mu_{\text{eff}}''/\mu_1'$. The effective permeabilities were

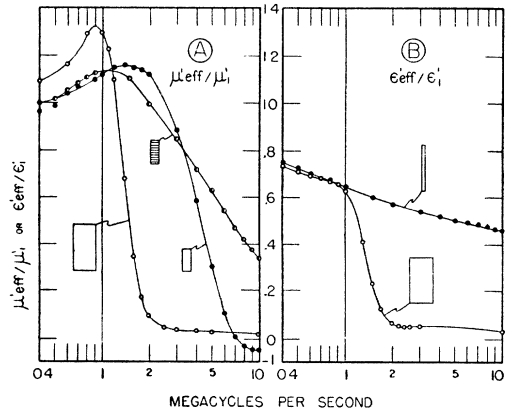

FIG. 2. Dependence of the real part of the effective material constants upon dimensions of the sample, experimental. Sample cross sections shown to scale for each curve. Data given as the ratio of the effective constant to the real part of the corresponding constant at 1000 c.p.s. A. Permeabilities. B. Dielectric constants.

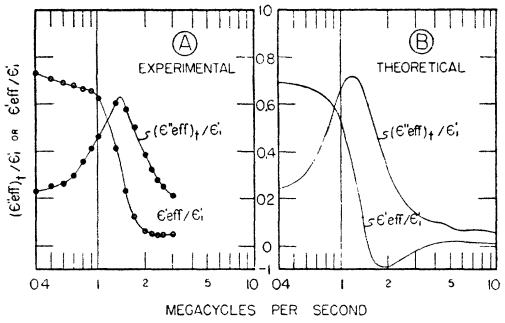

FIG. 3. Sample section 2.5×1.25 cm. A. Experimental values of the ratio of the effective dielectric constants to the real part of the actual dielectric constant at 1000 c.p.s. In the case of the imaginary part the influence of the conductivity has been removed. B. Theoretical values of the same.

computed according to Eqs. (8) in the theoretical section. μ_{eff}' increases to a maximum at about 0.9 mc and then decreases to a very low value at about 2 mc. In some samples, μ_{eff}' was observed to go negative in the neighborhood of this frequency.

When air gaps were introduced into the magnetic circuit,[4] the apparent resonance was shifted to higher frequencies. Because it is an experimental fact that one of the effects of the introduction of an air gap is to decrease the apparent losses of the inductor, another well-known method for reducing core losses was tried, i.e., to reduce the dimensions of the core in a direction perpendicular to the magnetic flux. Again it was found that the apparent resonance effects were pushed to higher frequencies. The shift to higher frequencies also occurred when the over-all core dimensions were not changed, but the core was laminated. The curve obtained with one of these laminations was substantially the same as with the core composed of ten laminations. (See Fig. 2A. In this figure the areas marked off are the core sections drawn to scale. The largest section is 2.5×1.25 cm.)

These phenomena indicated strongly that the deviations of μ_{eff}'/μ_1' from unity were not due alone to an inherent property of the material as would be the case if they were due only to magnetic resonance. Calculations on the effect of ohmic eddy currents indicated clearly that these alone could not account for the results and hence we were led to a consideration of the dielectric properties of the material.

[4] Experiments performed with air gaps at 1000 c.p.s. served to establish the fact that, when no intentional gaps were inserted in the core assembled as described, the faces of the bricks, which were in contact, were sufficiently plane and parallel so that no measurable effect upon the permeability could be observed. These experiments consisted in measuring the low frequency inductance of a given coil upon the core with the bricks pressed firmly together and then with various known gaps. When the reciprocals of the measured inductances were plotted against the gap lengths the line was straight and the intercept on the reciprocal inductance axis coincided with the reciprocal of the inductance measured when the blocks were pressed firmly together.

Dielectric Experiments

The dielectric properties of the material were investigated by applying, by evaporation, gold electrodes to opposite faces of appropriately shaped pieces.

The absence of electrode effects was demonstrated by showing the equality of the direct current resistivity if measured from the dimensions, the current through the electrodes and (a) the voltage drop across the electrodes or (b) the potential difference, measured potentiometrically, between two probe electrodes spaced along the direction of the current flow. Some further proof of the absence of electrode effects is that, with carefully applied electrodes, the low frequency (e.g., 1000 c.p.s. resistance between the electrodes was the same as the d.c. resistance observed.

The equivalent parallel reactance and resistance between the electrodes were measured from 200 to 100,000 c.p.s. on a fully-shielded equal-ratio-arm parallel impedance bridge. Above 100,000 c.p.s. the measurements were made as the equivalent series reactance and resistance between the electrodes, using either a General Radio 917 AL or 917 A Radio Frequency Bridge. These values were converted to equivalent parallel impedances by calculation. On account of the high dielectric constant of the material, no guard rings were necessary. The measured impedances were converted to effective

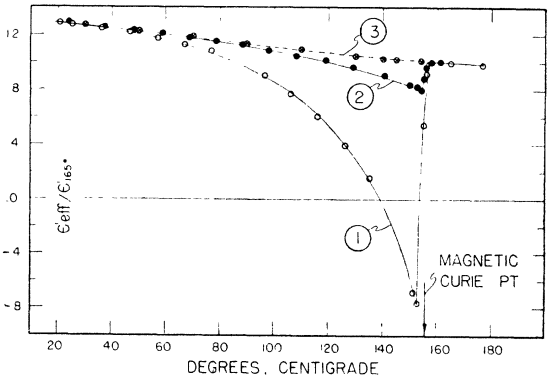

FIG. 4. The variation of the real part of the effective dielectric constant with temperature through the magnetic Curie point. Data plotted as the ratio of the effective constant to the real part of the actual constant at 165°C. (1) Sample section 2.5×1.25 cm. (2) Sample section 2.5×0.358 cm. (3) Actual dielectric constant computed from (2).

dielectric constants, ϵ_{eff}' and $(\epsilon_{\text{eff}}'')_t$, by means of Eqs. (8). In the effective dielectric loss factor, $(\epsilon_{\text{eff}}'')_t$, the effect of the ohmic current has been eliminated by means of Eq. (3).

Figure 3A shows the results for one of the 10 cm Ferroxcube III bricks, the electrodes being applied to the 2.5×1.25 cm ends. The results are plotted as the ratios of the effective constants to the real part of the actual dielectric constant at 1000 c.p.s.; i.e., $\epsilon_{\text{eff}}'/\epsilon_1'$ and $(\epsilon_{\text{eff}}'')_t/\epsilon_1'$. Again resonant effects are apparent and again, in the case of some bricks, we have observed

negative values of ϵ_{eff}' in the region of 2 mc. Figure 2B shows the effect on ϵ_{eff}' of reducing the 1.25 cm dimension to 0.127 cm. The areas marked off in the figure are the electrode areas drawn to scale. It is evident that resonant phenomena have been pushed to higher frequencies by making the sample thinner, as in the case of the magnetic permeability.

These experiments show conclusively that the material does have a dielectric behavior corresponding to a very high dielectric constant. The combination of the high dielectric constant and high magnetic permeability in the same material gives rise to the dimensional resonance which accounts for the anomalous results we have observed in our measurements of μ_{eff}' and ϵ_{eff}' in the samples of thicker section. A quantitative explanation will be given in the theoretical section.

When the unusual dielectric properties of the material were established, the question of the behavior of the dielectric properties as a function of temperature was investigated. Special interest was centered in the phenomena which occur at the magnetic Curie point.

The results given in Fig. 4 were obtained by measurements at 10,000 c.p.s. These data are plotted as the ratio of the real part of the effective dielectric constant at a given temperature to the real part of the dielectric constant at a temperature just above the magnetic Curie point. Curve 1 of this figure was obtained from measurements performed on a bar 1.25×2.50×10 cm with electrodes applied to the 1.25×2.50 cm faces. Curve 2 was obtained from a similar sample in which the 1.25 cm dimension was reduced to 0.358 cm and in which electrodes were applied to the 0.358×2.50 cm faces. The apparent dielectric constant for the thicker sample will be seen to become negative between about 138° and 154°C. The magnetic Curie point for the material studied is 155°C. Near this temperature (153°) the initial permeability rises to a rather sharp maximum and then falls rapidly to about 10 percent of its room temperature value at 156°. Throughout the entire temperature range, ϵ'' has no anomalies. It shows the same temperature dependence as does the conductivity. In Ferroxcube III, the conductivity varies with temperature in a manner common to semiconductors.

The apparent anomalies in the variation of the effective dielectric constant with temperature are explained in the theoretical section, and curve 3, obtained by correcting the data of curve 2 as discussed there, shows the course of the real part of the actual dielectric constant.

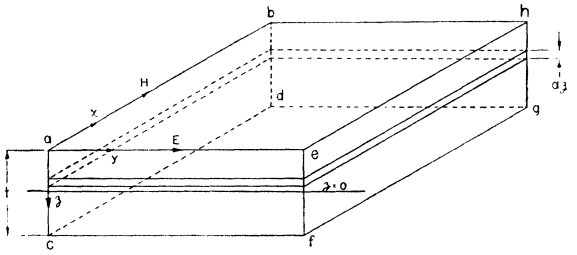

FIG. 5. Fundamental block of material used as the basis for the calculations in the theoretical section.

TABLE II. Actual material constants for samples used for the Curie point experiments.

	20°	150°	158°
Permeability, real part, μ'	1.4×10^3	2.6×10^3	<10
Permeability, imag. part, μ''	0	0	0
Dielectric constant, real part, ϵ'	9.5×10^4	7.5×10^4	7.5×10^4
imag. part, total, ϵ''	13.8×10^5	10.9×10^6	11.7×10^6
imag. part,* ϵ_t''	$\sim2.0\times10^4$	$\sim2.0\times10^4$	$\sim2.0\times10^4$
Conductivity (ohm cm)$^{-1}$, σ	7.5×10^{-3}	5.9×10^{-2}	6.3×10^{-2}

* Associated with true dielectric loss only.

In Table II are given, at three temperatures of interest, the actual material constants of the particular samples used for the investigation of the phenomena at the Curie point.

III. THEORETICAL

Derivation of the Impedance Expressions

Except for the limitations imposed by the assumed geometry, the following considerations are perfectly general and include many possible dimensional effects, of which dimensional resonance is a specific type. Other dimensional effects occur under non-resonant conditions, the ordinary shielding effect of ohmic eddy currents in magnetic cores being a case in point. All such effects lead to apparent material constants which differ in magnitude from the actual constants, are functions of the sample dimensions, and, in general, show a frequency dependence which is superimposed upon any frequency dependence existing in the actual constants.

Figure 5 shows a block of material to which a magnetic field H may be applied by means of a coil whose plane is parallel to the section *aecf* or an electric field E by means of electrodes on the faces *abcd* and *efgh*. Because of the relative simplicity of the resulting expressions, we have assumed H and E to vary only in the z-direction; i.e., perpendicular to the applied fields. This assumption imposes restrictions on the dimensions of the block or toroidal core of which, in the magnetic case, it is a part; i.e., (1) the thickness, t, must be small compared to the width of the section (*ab*, in the case of the dielectric block and *ae* in the case of the magnetic core), (2) the width must be small compared to the diameter of the toroid, (3) all dimensions must be small compared to the wave-length in vacuum of the electromagnetic wave set up by the applied fields. We shall be concerned, then, with dimensional effects connected with the dimension t only. The mathematics is essentially that of the "infinite slab."

Referring to Fig. 5, we take $z=0$ to be the center of the block section for reasons of symmetry. For the

magnetic core, the boundary condition is that at both surfaces, *abhe* and *cdgf*, the magnetizing field reduces to what it would be at zero frequency, H_s. Similarly, for the dielectric block, the electric field at these same surfaces reduces to E_s, the value it would have at zero frequency. Under these conditions, the Maxwell equations lead to the following solutions when the time variations of the various quantities are taken to be sinusoidal.

$$H=H_s\frac{\cos jkz}{\cos jkt/2},\quad E=E_s\frac{\cos jkz}{\cos jkt/2}. \tag{1}$$

Here $k=j\omega\mu^{\frac{1}{2}}\epsilon^{\frac{1}{2}}/c$ and is the propagation constant of the electromagnetic wave in the core.

The impedance of the reactor, of which the magnetic core is a part, is found from the ratio of applied voltage to current, V_m/I_m where $V_m\sim\omega\int Hdz$ and $I_m\sim H_s$. Similarly, the admittance of the condenser formed by the dielectric block is found from the ratio I_d/V_d where $I_d\sim\omega\int Edz$ and $V_d\sim E_s$. When these operations are carried out, we have

Reactor impedance

$$Z_m=-(2c^2/\omega)K(k/\epsilon)\tan jkt/2, \tag{2}$$

Condenser admittance

$$Y_d=2Q\omega(\epsilon/k)\tan jkt/2.$$

Here $K=L/\mu t$ and $Q=C/\epsilon t$ where L is the ordinary low frequency inductance of the reactor and C is the ordinary low frequency capacity of the condenser. K depends only on the number of turns and dimensions of the reactor; Q only on the dimensions of the condenser. With L in henries, C in farads, and all other quantities in the c.g.s. system, Z_m is in ohms and Y_d in mhos.[5] For some calculations, it is convenient to replace ϵ/k in Eqs. (2) by $-c^2k/\omega^2\mu$.

The general expressions for Z_m and Y_d can now readily be derived from (2) by making the substitutions $\mu=\mu'-j\mu''$ and $\epsilon=\epsilon'-j\epsilon''$ where μ'' accounts for losses associated with the magnetization and ϵ'' for losses connected with currents flowing in the material. A detailed consideration of Maxwell's equations shows that ϵ'' may be separated into factors accounting for dielectric losses alone, ϵ_t'', and for ohmic losses alone; i.e.

$$\epsilon''=\epsilon_t''+4\pi\sigma c^2 10^{-9}/\omega, \tag{3}$$

where σ is in (ohm-cm)$^{-1}$. It is convenient to carry ϵ'' alone throughout the calculations. The true dielectric loss factor can then at any time be found by determining σ from d.c. measurements and substitution in (3).

[5] In terms of the dimensions of the reactor core and block, $K=4\pi n^2 w10^{-9}/l$ and $Q=w10^9/4\pi c^2 l$. Here w is the width of core or block section and l the mean flux path of the core or distance between electrodes of the block. When these expressions for K and Q are used, Z_m comes out in ohms and Y_d in mhos.

By inserting the complex values of μ and ϵ, we find $k=\alpha+j\beta$ where

$$\begin{aligned}\alpha&=(\omega/c\sqrt{2})\{(\mu'^2+\mu''^2)^{\frac{1}{2}}(\epsilon'^2+\epsilon''^2)^{\frac{1}{2}}-(\mu'\epsilon'-\mu''\epsilon'')\}^{\frac{1}{2}},\\ \beta&=(\omega/c\sqrt{2})\{(\mu'^2+\mu''^2)^{\frac{1}{2}}(\epsilon'^2+\epsilon''^2)^{\frac{1}{2}}+(\mu'\epsilon'-\mu''\epsilon'')\}^{\frac{1}{2}}.\end{aligned} \tag{4}$$

It should be remembered that in general there is, by virtue of (3), a frequency term under the radical in (4), even though all material constants are independent of frequency. Physically α is the extinction coefficient and ω/β gives the phase velocity of the electromagnetic wave in the material. These quantities appear in the ordinary wave equation thus,

$$E=E_0\{\exp-\alpha x\}\{\exp j\omega(\tau-\beta x/\omega)\}.$$

By taking the real and imaginary parts of (2) after inserting the complex values of μ and ϵ, the following expressions are obtained.

$$\begin{aligned}R_m&=\frac{2K\omega}{\alpha^2+\beta^2}\left\{\frac{B\sinh\alpha t-A\sin\beta t}{\cosh\alpha t+\cos\beta t}\right\},\\ X_m&=\frac{2K\omega}{\alpha^2+\beta^2}\left\{\frac{A\sinh\alpha t+B\sin\beta t}{\cosh\alpha t+\cos\beta t}\right\},\end{aligned} \tag{5}$$

$$\begin{aligned}r_d&=\frac{\omega}{2c^2Q}(\mu'^2+\mu''^2)\left\{\frac{\cosh\alpha t+\cos\beta t}{B\sinh\alpha t+A\sin\beta t}\right\},\\ x_d&=\frac{\omega}{2c^2Q}(\mu'^2+\mu''^2)\left\{\frac{\cosh\alpha t+\cos\beta t}{A\sinh\alpha t-B\sin\beta t}\right\},\end{aligned} \tag{6}$$

where

$$A=\mu'\alpha-\mu''\beta,\quad B=\mu'\beta+\mu''\alpha,\quad R_m+jX_m=Z_m$$

and

$$1/r_d+1/jx_d=Y_d.$$

These expressions are rigorous and automatically carry the proper sign so that if any reactance term turns out to be positive an inductive reactance is denoted and if negative, a condensive reactance. It should be noted that R_m and X_m are the equivalent series resistance and reactance of the reactor while r_d and x_d are the equivalent parallel resistance and reactance of the condenser. For some calculations it may be convenient to change the coefficients of the transcendental terms in (5) and (6) according to the following identities.

$$\frac{\omega^2}{c^2}\left(\frac{\mu'^2+\mu''^2}{B}\right)\equiv\frac{\alpha^2+\beta^2}{B'},\quad \frac{\omega^2}{c^2}\left(\frac{\mu'^2+\mu''^2}{A}\right)\equiv-\frac{\alpha^2+\beta^2}{A'},$$

where $A'=\epsilon'\alpha-\epsilon''\beta$ and $B'=\epsilon'\beta+\epsilon''\alpha$. Alternate expressions for the impedances may also be derived in terms of $\Re\tan jkt/2$ and $\Im\tan jkt/2$ explicitly. (See reference 8.)

Equations (5) and (6) contain many special cases of importance. For example, when ϵ', ϵ_t'', and μ'' are

neglected, Eqs. (5) reduce to those developed by K. L. Scott[6] for the case of a reactor with ohmic eddy currents alone. In this case α becomes equal to β and is the reciprocal of the ordinary penetration depth. Other special cases will be discussed in the section on effects at the Curie point.

Effective *vs.* Actual Material Constants

From the definitions of the various quantities involved, apparent or effective material constants can be determined. These play the roles of the actual constants for any particular reactor or condenser and any particular frequency under consideration but have no general interest. It is, however, convenient to use the effective values when discussing a particular experiment. In the absence of dimensional effects, the effective constants will be equal to the respective actual constants. The effective values can be obtained from the fundamental impedance and admittance equations,

$$Z_m = jK\omega t\mu_{\text{eff}} \quad \text{and} \quad Y_d = jQ\omega t\epsilon_{\text{eff}}$$

giving

$$\mu_{\text{eff}} = -jZ_m/K\omega t \quad \text{and} \quad \epsilon_{\text{eff}} = -jY_d/Q\omega t. \tag{7}$$

In general, these quantities are complex and their components can be determined directly from measured values of the impedances.

$$\begin{aligned} \mu_{\text{eff}}' &= X_m/K\omega t, \qquad \mu_{\text{eff}}'' = R_m/K\omega t, \\ \epsilon_{\text{eff}}' &= -1/x_dQ\omega t, \qquad \epsilon_{\text{eff}}'' = 1/r_dQ\omega t. \end{aligned} \tag{8}$$

By substituting (5) and (6) in (8), the effective constants can be calculated rigorously from the actual material constants.

Determination of the Actual Values of μ', μ'', ϵ' and ϵ'' from Measured Values of the Impedances

Although Eqs. (8) with X_m, R_m, x_d, r_d substituted from (5) and (6) can, in principle, be solved for rigorous explicit expressions for the actual material constants in terms of the effective constants, these expressions would be cumbersome and it is simpler to return to Eqs. (2) and proceed in a somewhat circuitous way. In the following outline it is assumed that the equivalent series reactance and resistance of the reactor and the equivalent parallel reactance and resistance of the condenser have been measured, i.e. X_m, R_m, x_d, r_d. The relative dimensions of the reactor core and dielectric block are immaterial except that the thickness, t, of the two must be the same and that the before-mentioned limiting conditions are met.

Multiplying Eqs. (2) together leads to the following rigorous expressions from which α and β can be calculated.

$$\begin{aligned} \tan\beta t &= -2\Phi D/\{D^2-(\Psi^2+\Phi^2)\}, \\ \sinh\alpha t &= 2\Psi D/[\{D^2-(\Psi^2+\Phi^2)\}^2+4\Phi^2D^2]^{\frac{1}{2}}, \end{aligned} \tag{9}$$

where

$$\begin{aligned} \Phi &= \mp(1/\sqrt{2})\{(p^2+q^2)^{\frac{1}{2}}-p\}^{\frac{1}{2}}; \\ \Psi &= (1/\sqrt{2})\{(p^2+q^2)^{\frac{1}{2}}+p\}^{\frac{1}{2}}; \end{aligned}$$

$p = R_m/r_d + X_m/x_d$; $\quad q = X_m/r_d - R_m/x_d$; $\quad D = 2cK^{\frac{1}{2}}Q^{\frac{1}{2}}$; and Φ takes the sign opposite to q. Care must be taken to insert the values of X_m and x_d, in these expressions, with their proper signs. At a sufficiently low frequency, X_m will be positive and x_d negative. Care must also be taken that βt is chosen in the proper quadrant. In general, a series of measurements at various frequencies will be necessary to establish the proper course of βt. Having the values of αt and βt, the actual dielectric constants can be calculated as follows:

When Eqs. (6) are substituted in (8), the resulting expressions can be solved for ϵ' and ϵ'', giving

$$\begin{aligned} \epsilon' &= \epsilon_{\text{eff}}'U(V+\epsilon_{\text{eff}}''W/\epsilon_{\text{eff}}'), \\ \epsilon'' &= \epsilon_{\text{eff}}''U(V-\epsilon_{\text{eff}}'W/\epsilon_{\text{eff}}''), \end{aligned} \tag{10}$$

where

$$\begin{aligned} U &= (\cosh\alpha t+\cos\beta t)/2(\sinh^2\alpha t+\sin^2\beta t), \\ V &= \alpha t\sinh\alpha t+\beta t\sin\beta t, \\ W &= \beta t\sinh\alpha t-\alpha t\sin\beta t. \end{aligned}$$

In using Eqs. (10), αt and βt are obtained from (9) while ϵ_{eff}' and ϵ_{eff}'' are determined from measured quantities using (8). When the value of ϵ'' has been determined from (10), ϵ_t'' can be computed from (3) in which σ is known from d.c. measurements. The expressions for the actual permeabilities are the same as (10) except that, where they occur explicitly, the ϵ's are replaced by the corresponding μ's. For the calculation of either the ϵ's or the μ's, the factors U, V, W remain the same. (See discussion of Eq. (12) in the section Approximate Expressions. Also in this section, approximations are developed for Eqs. (10).)

Numerical Calculations of the Actual Core Constants

The actual material constants in c.g.s. units are given in Fig. 6, as calculated from the rigorous expressions, using impedance measurements on samples of the following dimensions:

Magnetic toroid: Section, 0.127×0.53 cm; mean flux path, 5.56 cm.
Dielectric block: Section, 0.127×2.5 cm; length, 7 cm.

In this case, the 0.127 cm thickness of the section was taken as determining the dimensional effects. At 10 mc, the maximum effect in any of the constants occurs in ϵ'', where $\epsilon''/\epsilon_{\text{eff}}'' = 0.69$. Above 10 mc, our measurements become unreliable because of the difficulty of estimating with sufficient accuracy the distributed capacity effects

[6] K. L. Scott, Proc. I.R.E. **18**, 1750 (1930).

in the magnetic measurements. Below 10 mc we have been able to correct for such effects. While some corrections may still have to be applied because of geometrical limitations, we believe these will be small. It is evident that a considerable dispersion remains after removal of the dimensional effects, particularly in the magnetic constants. The dependence of the components of the propagation constant on frequency is given in Fig. 6B.

The results of calculating the effective constants for $t=1.25$ cm from the actual constants of Fig. 6, using the rigorous equations, are given in Figs. 1B and 2B. Here they are shown in comparison to experimental values on core and block sections 1.25×2.5 cm. We believe the discrepancies are due, in large part, to the failure of these experimental samples of relatively thick section to satisfy sufficiently well the geometrical limitations. As mentioned in the experimental section, on some samples of Ferroxcube III of these dimensions, we have observed negative values of both μ' and ϵ' in the vicinity of 2 mc. In none of these cases, however, are complete measurements available for the determination of the actual material constants. The values of the effective constants in the resonant region are rather sensitive to both the geometry of the core[7] and the actual material constants.

Calculations have also been made on the effect of an air gap in the magnetic core, using Eqs. (5). In making the calculations, the value of the permeability used was the actual value as reduced by the air gap. Reasonable agreement with experiment was obtained.

It should be emphasized that the major features of such curves as Figs. 1B and 2B are not necessarily determined by a dispersion of the actual core constants. Figures 7A and 7B show similar results, for example, when the actual core constants are taken to be independent of frequency.

Magnetic Flux Distribution

The magnetic flux distribution in the core of the reactor is found from (1) by multiplying by the permeability, $\mu'-j\mu''$. Two standing wave patterns result, differing in phase from each other by 90°. The real pattern, $\Re\mathbf{B}$, is associated with the reactance of the reactor and the imaginary pattern, $\Im\mathbf{B}$, with its effective resistance. The total flux, $\mathbf{B}_{\text{tot}}$ is the vector sum of the two patterns. Following are the expressions for the flux distributions.

$$\Re\mathbf{B}=H_s\frac{\mu'S+\mu''T}{\cosh\alpha t+\cos\beta t},\quad \Im\mathbf{B}=H_s\frac{\mu'T-\mu''S}{\cosh\alpha t+\cos\beta t},\qquad (11)$$

[7] We have, for example, derived the equations for the effective constants for samples of circular cross section and find the resonance phenomena move to higher frequencies when the diameter of the circular section is the same as the thickness of the "infinite slab."

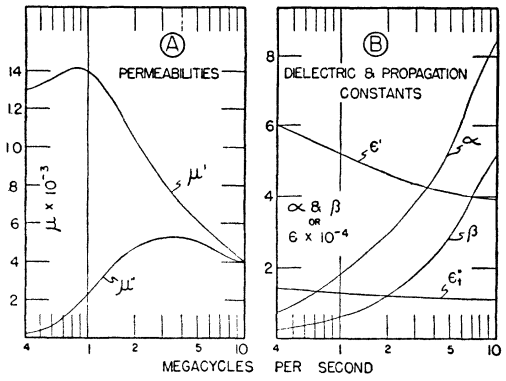

FIG. 6. Actual material constants for Ferroxcube III. A. Permeabilities. B. Dielectric constants. Propagation constants in cm^{-1} for an electromagnetic wave.

where

$$S=\cos\beta(z+t/2)\cosh\alpha(z-t/2)+\cos\beta(z-t/2)\cosh\alpha(z+t/2),$$
$$T=\sin\beta(z-t/2)\sinh\alpha(z+t/2)+\sin\beta(z+t/2)\sinh\alpha(z-t/2).$$

Figure 8 shows these distributions, calculated for the frequency where the reactance first becomes zero in Fig. 7A. Since at the surfaces, $\mathbf{B}=\mu H_s$ and μ'' has been taken to be zero, $\Im\mathbf{B}$ reduces to zero at the surfaces while $\Re\mathbf{B}$ reduces to $\mu' H_s$. The integral of $\Re\mathbf{B}$ across the core section accounts for the reactance of the coil and is zero as it should be for this particular case. It is noteworthy that the total flux density is actually higher within the core than at the surface. To speak of the penetration depth of the flux is obviously meaningless in this case. Similar considerations apply to the distribution of the electric intensity in the dielectric block.

Approximate Expressions

For purposes of approximation, Eqs. (2) can be substituted in (7) and $\tan jkl/2$ developed directly. This

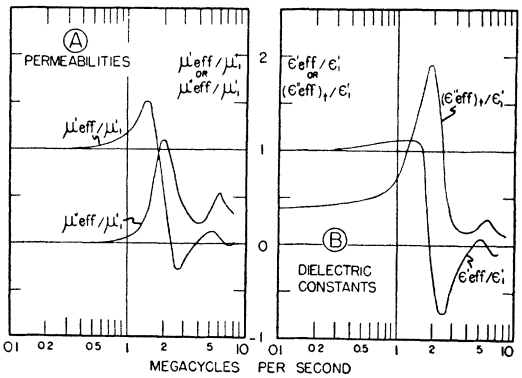

FIG. 7. Effective material constants calculated for sample thickness 1.25 cm assuming actual material constants independent of frequency. $\mu'=10^3$, $\mu''=0$, $\epsilon'=5\times10^4$, $\epsilon_t''=2\times10^4$, $\sigma=5\times10^{-3}$. A. Permeabilities. B. Dielectric constants.

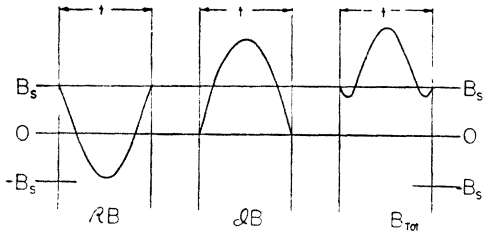

FIG. 8. Flux distribution in the core of Fig. 7A at a frequency where μ_{eff}' has its first zero.

procedure gives

$$\mu_{eff}=\mu\left[1-\left\{\frac{(kt)^2}{12}-\frac{(kt)^4}{120}+\cdots\right\}\right],$$
$$\epsilon_{eff}=\epsilon\left[1-\left\{\frac{(kt)^2}{12}-\frac{(kt)^4}{120}+\cdots\right\}\right]. \tag{12}$$

These equations show clearly the symmetry between expressions for μ_{eff} and ϵ_{eff}. For example, expressions for μ_{eff}' and μ_{eff}'' are obtained from the expressions for ϵ_{eff}' and ϵ_{eff}'' when the ϵ's are replaced, where they occur explicitly, by the corresponding μ's. In the following, then, we shall write only expressions for the ϵ's.

When the complex value for ϵ is inserted in (12) and only the terms of second degree in αt and βt are retained, the effective constants are given by

$$\epsilon_{eff}'=\epsilon'\left[(1-M)-\frac{\epsilon''}{\epsilon'}N\right],$$
$$\epsilon_{eff}''=\epsilon''\left[(1-M)+\frac{\epsilon'}{\epsilon''}N\right], \tag{13}$$

where

$$M=\frac{(\alpha^2-\beta^2)t^2}{12} \quad \text{and} \quad N=\frac{\alpha\beta t^2}{6}.$$

When α and β are substituted in (13) in terms of the actual constants, we have

$$\epsilon_{eff}'=\epsilon'\left[1+\frac{\omega^2t^2}{12c^2}\left\{\frac{\mu'}{\epsilon'}(\epsilon'^2-\epsilon''^2)-2\mu''\epsilon''\right\}\right],$$
$$\epsilon_{eff}''=\epsilon''\left[1+\frac{\omega^2t^2}{12c^2}\left\{\frac{\mu''}{\epsilon''}(\epsilon'^2-\epsilon''^2)+2\mu'\epsilon'\right\}\right]. \tag{14}$$

Equations (13) may be solved for the actual constants, giving

$$\epsilon'=\epsilon_{eff}'\left[(1-M)+\frac{\epsilon_{eff}''}{\epsilon_{eff}'}N\right]\Big/\left[(1-M)^2+N^2\right],$$
$$\epsilon''=\epsilon_{eff}''\left[(1-M)-\frac{\epsilon_{eff}'}{\epsilon_{eff}''}N\right]\Big/\left[(1-M)^2+N^2\right]. \tag{15}$$

These last equations have the same form as the rigorous Eqs. (10). The approximate expressions for the factors $U\cdot V$ and $U\cdot W$, appearing in (10), can thus be determined from (15) by inspection.

In using these approximations, care must be taken to see that the approximation is warranted. When the actual material constants are complex, the degree of approximation is not a function of $|kt|$ alone as might be inferred from a casual inspection of (12). Actually in arriving at (13), (14), and (15) it is $\tan jkt/2$ which is being approximated. Retaining second degree terms in αt and βt in (12) is equivalent to retaining third degree terms in αt and βt in the development of $\tan jkt/2$. This latter is a very good approximation. For example, so long as αt and βt are each no greater than unity, the error in neither component of $\tan jkt/2$ can be more than about 5 percent. If αt and βt are each no greater than 0.8, the error can be no more than about 1.5 percent. These errors may, however, be greatly magnified in computing the effective material constants. This is because one or the other of the effective constants can always be written rigorously as the difference between two terms; i.e., as $P\cdot\Re\tan jkt/2-Q\cdot\Im\tan jkt/2$, where P and Q are functions of αt, βt and the actual material constants appearing explicitly.[8] When approximate expressions for $\tan jkt/2$ are used, the resulting percentage error in this effective constant is influenced by the ratio of the two terms; i.e., by

$$\chi=(\mu''\beta-\mu'\alpha)\sinh\alpha t/(\mu'\beta+\mu''\alpha)\sin\beta t.$$

As χ approaches unity, the merit of the approximation for the effective constants becomes poorer and the approximation is good only for very small values of αt and βt. Conversely, the merit becomes better when χ approaches zero and the approximation for the effective constants then approaches that for $\tan jkt/2$ itself. Similar considerations apply to the merit of the approximation for the actual constants in Eq. (15). The ratio, χ, is the same as before except that the effective constants replace the actual constants where they occur explicitly.

It should be emphasized further that the presence or absence of dimensional effects does not, as might be inferred from (12), depend on $|kt|$ alone. This is shown by Eqs. (13) where, because of the factor ϵ''/ϵ' or ϵ'/ϵ'', one or the other of the effective constants may differ greatly from the corresponding actual constant, even though αt and βt are each small compared to unity. Under these conditions, the dimensional effects will be important in ϵ_{eff}' if $\epsilon''\gg\epsilon'$ and in ϵ_{eff}'' if $\epsilon''\ll\epsilon'$.

[8] When the effective constants are expressed in this way as functions of $\Re\tan jkt/2$ and $\Im\tan jkt/2$, they may be calculated from tables of these quantities instead of using tables of hyperbolic and circular functions as when working with expressions derivable from (5) and (6). (See Kennelly, *Tables of Complex Hyperbolic and Circular Functions* (Harvard University Press, Cambridge, 1914).) The tables of the tangent of a complex variable can also be used in estimating the errors introduced by approximations of $\tan jkt/2$.

Effects at the Magnetic Curie Point

When the material is carried through the magnetic Curie point, the effective dielectric constant, measured at 10^4 c.p.s. on relatively thick blocks, shows the rather interesting behavior described in the experimental section. Significant dimensional effects are present, even at these relatively low frequencies where there can be no question of dimensional resonance. Some sort of discontinuity is naturally to be expected at the Curie point because of the collapse of the permeability. The rather rapid decline of the effective dielectric constant with increasing temperature below the Curie point, however, has no primary connection with the permeability. It arises, instead, from the fact that the conductivity of Ferroxcube III increases rapidly with temperature.

Calculations from the data of Table II show that the maximum dimensional effects are to be expected just below the Curie point (155°C), where ϵ''/ϵ', αt and βt have relatively large values; i.e. $\alpha t \cong \beta t \cong 0.15$ for a block 1.25 cm thick and $\epsilon''/\epsilon' \cong 150$. Under these conditions the approximations retaining only the second degree terms in αt and βt can be used safely. The second degree terms, however, lead to large dimensional effects, Since $\mu'' \cong 0$ and $\epsilon_t'' \ll \epsilon''$, further approximation in (14). which retains the second degree terms, is warranted and we may write:

$$\epsilon_{\text{eff}}' = \epsilon' \left\{ 1 - \frac{4}{3}\pi^2 \frac{\mu'}{\epsilon'} t^2 \sigma^2 c^2 \cdot 10^{-18} \right\}, \tag{16}$$

$$\epsilon_{\text{eff}}'' = \epsilon'' = 4\pi\sigma c^2 \cdot 10^{-9}. \tag{17}$$

Equation (17) shows at once that no appreciable discontinuity in ϵ''_{eff} is to be expected at the Curie point. On the other hand, Eq. (16) shows a marked effect of the permeability depending upon the magnitude of $(t\sigma)^2/\epsilon'$.

Just below the Curie point, the difference between ϵ_{eff}' and ϵ' is large and is influenced by the square of the conductivity. Since the latter is a rapid function of the temperature, ϵ_{eff}' becomes very sensitive to temperature changes. In fact it is not difficult to cause ϵ_{eff}' to become negative just below the Curie point, as shown in Fig. 4. At the Curie point, ϵ_{eff}' will suffer a near discontinuity owing to the sudden collapse of μ'. Above the Curie point, since μ' is now small, there is little difference between ϵ_{eff}' and ϵ' and further changes in the conductivity caused by further increase in temperature will have little effect.[9]

Like all dimensional effects, these phenomena at the Curie point can be made negligible by making measurements on a sample sufficiently thin. ϵ_{eff}' then approaches ϵ' in value throughout the entire temperature range. Otherwise ϵ' can be determined from Eq. (16) as

$$\epsilon' = \epsilon_{\text{eff}}' + (4/3)\pi^2 \mu' t^2 \sigma^2 c^2 \cdot 10^{-18}. \tag{18}$$

ϵ' as computed from (18) using the data of curve 2, Fig. 4, is shown as curve 3, Fig. 4. Equation (18) does not give as satisfactory a correction for curve 1 of Fig. 4, not because the approximation is invalid but because the geometrical limitations of our theory are not met as well by the thicker block.

IV. ACKNOWLEDGMENTS

We wish to extend our thanks to Dr. O. S. Duffendack and Dr. F. K. du Pré of this Laboratory, to Dr. H. M. Blewett of the Brookhaven Laboratory, and to Professor G. E. Uhlenbeck for their advice and criticism.

---

[9] Low frequency dimensional effects in the dielectric block can also be discussed in terms of an equivalent circuit for the block. In the case of our Curie point experiment, this circuit consists of two parallel impedances. One is that of the block considered as a lossless condenser (permeability taken as unity); the other is that of the block considered as a lossless inductor (dielectric constant taken as unity) in series with a resistance (the d.c. resistance of the block). The impedance of the inductive branch can be calculated from $1/Y_d = (2Q\omega)^{-1} k\epsilon^{-1} \cot jkt/2$. When this is developed in the same way as we developed Z_m and Y_d and we put $\epsilon' = 1$, $\epsilon_t'' = \mu'' = 0$, the inductance comes out to be $\mu'/12c^2Q$ henries to the same degree of approximation used in Eqs. (14). Here we have neglected the inductance arising from the field external to the block. Now, when the equivalent circuit is converted to a reactance shunted by a resistance, as it is measured, Eqs. (16) and (17) result. In the conversion, the further approximation is made that in the inductive branch of the equivalent circuit, the resistance is large compared to the reactance. An explanation of the Curie point phenomena in essentially this manner, was given independently by C. G. Koops of the Philips Laboratory, Eindhoven, in a private communication to the authors.